Bearing Capacity of Strip Footing in Two-Layer $c-\varphi$ Soils Exhibiting Anisotropy and Nonhomogeneity in c

by

A. Siva Reddy*
K.N. Venkatakrishna Rao**

Introduction

Most natural deposits are anisotropic and nonhomogeneous with respect to shear strength (Casagrande and Carillo, 1944; Lo, 1965; Bishop, 1966; Livneh and Komornik 1967). In addition to nonhomogeneity in cohesion, nonhomogeneity in the form of layers is of common occurrence. Several experimental, theoretical and semiemperical methods with regard to layered soils have been reported in literature (Button, 1953; Yamaguchi, 1963; Reddy and Srinivasan, 1967; Stragnov, 1967; Brown and Meyerhof, 1969; Meyerhof, 1974; Purushothamaraj, Ramiah and Venkatakrishna Rao, 1974; Vesic 1975; Tejchmen, 1977; Meyerhof and Hanna, 1978; Hanna and Meyerhof, 1979). For the case of two layered $c-\varphi$ soils, in the studies that have been reported so far, the soil in each layer is treated as isotropic and homogeneous. But, in nature the soil in each layer could be anisotropic and nonhomogeneous. Of the several analytical methods of finding the bearing capacity of soil, limit analysis, particularly upper bound analysis, is found to be a convenient tool (Chen, 1975). In this analysis, the ultimate bearing capacity of strip footing on a two layer $c-\varphi$ soil is obtained using limit analysis. A Prandtl-Terzaghi failure mechanism with varying boundary wedge angles is assumed and soil in each layer is assumed to have same angle of internal friction. The results are presented in the form of charts in terms of nondimensional quantities.

Analysis

The two layer system considered in this analysis is shown in Fig. 1 and the various parameters are defined in the list of notations. The

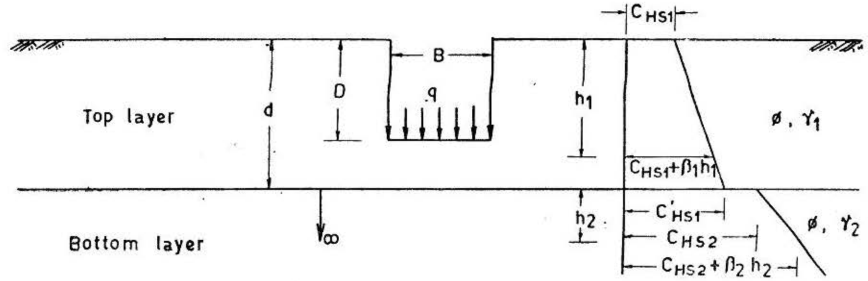

FIGURE 1 Two Layer System Considered in the Analysis

*Professor of Civil Engineering, Indian Institute of Science, Bangalore, 560 012, India.

**Assistant Professor of Civil Engineering, Government BDT College of Engineering, Davanagere, 577 004, India.

(This paper was received in May 1982, and is open for discussion till end of April 1984)

Prandtl-Terzaghi type failure mechanism is assumed. For given parameters d, D, B and φ, the angles ξ and η define the failure surface (Fig. 2(a)). Depending on the values of the parameters and the values of ξ and η, different cases of failure arise. These cases are :

(i) Case 1 : the central wedge lies entirely in the top layer

$$\left[d \geqslant \left(D+\frac{B}{2}\tan\xi\right)\right],$$

(ii) Case 2 : the central wedge extends to bottom layer

$[d > D < (D+B/2 \tan \xi)]$, and

(iii) Case 3 : the central wedge lies entirely in the bottom layer $d < D$.

In case 1, two further cases will arise, viz.,

(a) Case 1A; the η line lies in top and bottom layers (Fig. 2(a)) and

(b) Case 1B; the η line lies entirely in the top layers (Fig. 2(b)).

In case 2 also, two further cases arise, viz.,

(a) Case 2A; the η line lies in both the top and bottom layers (Fig. 3(a)) and

(b) Case 2B; the η line lies entirely in the top layer (Fig. 3(b)).

For case 3, the failure mechanism is shown in Fig. 4. The analysis for case 1A is presented below.

The velocity triangle is shown in Fig. 2a and the velocities V_1 and V_r are given by

$$V_1 = \text{vertical velocity} = \frac{V_0 \cos\varphi}{\cos(\xi-\varphi)} \qquad \dots (1)$$

$$V_r = \text{relative velocity along } bc = \frac{V_0 \sin\xi}{\cos(\xi-\varphi)} \qquad \dots (2)$$

where V_0 = relative velocity at point c along log spiral (see Fig. 2(a)). The cohesion is assumed to vary linearly with depth (see Fig. 1) and the soil is assumed to be anisotropic. The variation of cohesion with direction is taken as

$$c_i = c_H + (c_V - c_H)\sin^2 i \qquad \dots (3)$$

Referring to Fig. 2a, the rate of energy dissipation along $bc = E_1$

$$E_1 = (\text{average } c_i \text{ along } bc)\,(\text{length } bc)\,(V_r \cos\varphi)]$$

$$= \left[c_{HS1}+\beta_1 D+\frac{\beta_1 B}{4}\tan\xi\right]\left[1+(k_1-1)\sin^2(\xi+\mu)\right] \cdot \left[\frac{BV_0 \sin\xi\cos\varphi}{2\cos\xi\cos(\xi-\varphi)}\right] \qquad \dots (4)$$

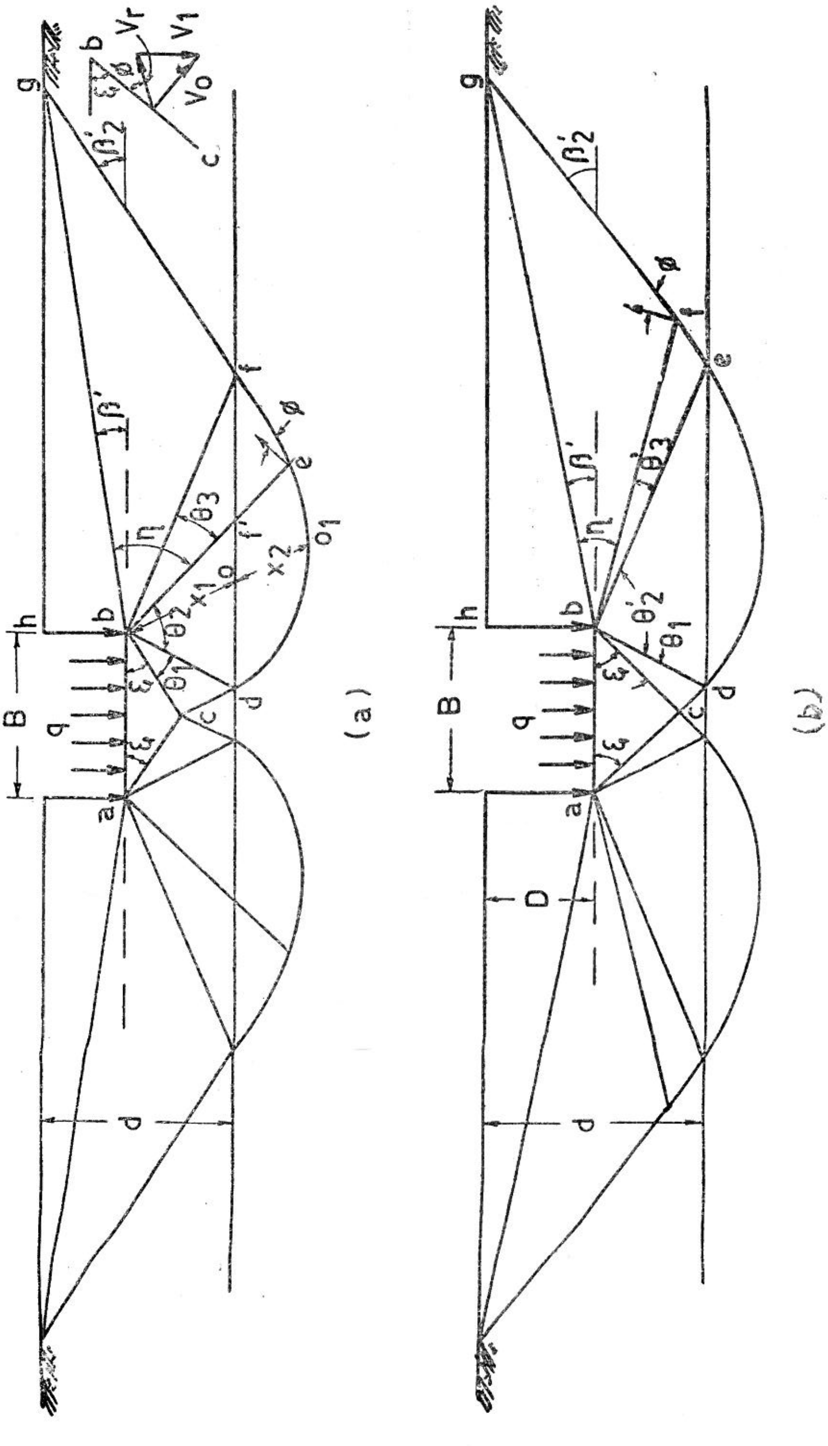

FIGURE 2 Failure Mechanism (*a*) Case 1*A* (*b*) Case 1*B*

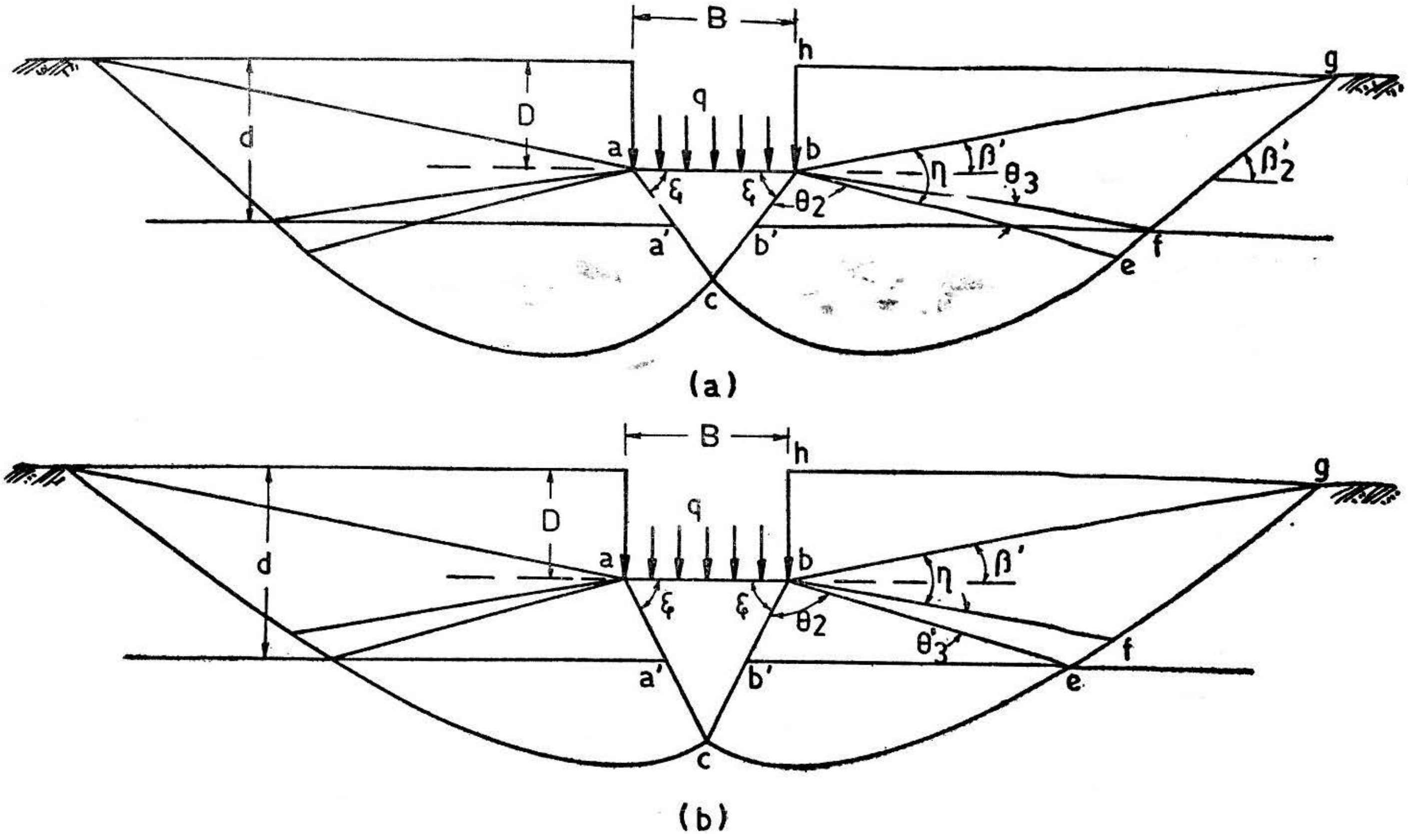

FIGURE 3 Failure Mechanism (*a*) Caes 2*A* (*b*) Case 2*B*

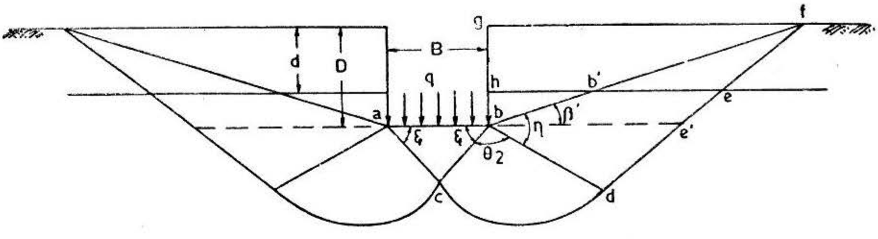

FIGURE 4 Failure Mechanism—Case 3

Rate of energy dissipation in the portion bcd of the logarithmic spiral $= E_2$

$$E_2 = \int_0^{\theta_1} (\text{average } c_i \text{ along a radial line}) \, (V_r \, d\theta)$$

$$= (c_{HS1} + \beta_1 D) \left[\int_0^{\theta_1} e^{2\theta \tan \varphi} \, d\theta \right.$$

$$\left. + (k_1 - 1) \int_0^{\theta_1} e^{2\theta \tan \varphi} \sin^2 (\xi + \theta + \mu) \, d\theta \right]$$

$$+ \frac{\beta_1 B}{4 \cos \xi} \left[\int_0^{\theta_1} e^{3\theta \tan \varphi} \sin (\xi + \theta) \, d\theta \right.$$

$$\left. + (k_1 - 1) \int_0^{\theta_1} e^{3\theta \tan \varphi} \sin (\xi + \theta) \sin^2 (\xi + \theta + \mu) \, d\theta \right] \frac{BV_0}{2 \cos \xi} \quad \ldots (5)$$

Rate of energy dissipation along logarithmic spiral $cd = E_3$

$$E_3 = \int_0^{\theta_1} (c_i \text{ at a point on logarithmic spiral}) \, (V_r \, d\theta)$$

$$= (c_{HS1} + \beta_1 D) \left[\int_0^{\theta_1} e^{2\theta \tan \varphi} \, d\theta + (k_1 - 1) \int_0^{\theta_1} e^{2\theta \tan \varphi} \, d\theta \right.$$

$$+ (k_1 - 1) \int_0^{\theta_1} e^{2\theta \tan \varphi} \sin^2 (X - \theta) \, d\theta$$

$$+ \frac{\beta_1 B}{2 \cos \xi} \int_0^{\theta_1} e^{3\theta \tan \varphi} \sin (\xi + \theta) \, d\theta$$

$$\left. + (k_1 - 1) \int_0^{\theta_1} e^{3\theta \tan \varphi} \sin (\theta + \xi) \sin^2 (X - \theta) \, d\theta \right] \frac{BV^0}{2 \cos \xi} \quad \ldots (6)$$

where, $X = 90 + \varphi + \mu - \xi$

Rate of energy dissipation along de is given by E_4

$$E_4 = \int_0^{\theta_2} (c_i \text{ along } de)\,(V_r\, d\theta)$$

$$= \int_0^{\theta_2} c_{HS_2} + \beta_2 \left[\frac{B}{2\cos\xi}\, e^{(\theta_1+\theta)\tan\varphi} - \frac{(d-D)}{\sin(\xi+\theta_1+\theta)} \right]$$

$$. \sin(\xi+\theta_1+\theta)\,[1+(k_2-1)\sin^2(Y-\theta)]$$

$$\left[\frac{BV_0}{2\cos\xi}\, e^{2(\theta_1+\theta)\tan\varphi} \right] d\theta \qquad \ldots (7)$$

where

$$Y = 90+\varphi+\mu-\xi-\theta_1$$

Rate of energy dissipation in the region bde can be written as E_5

$$E_5 = \int_0^{\theta_2} [\,(\text{average } c_i \text{ in portion } x_1)\, x_1$$

$$+(\text{average } c_i \text{ in portion } x_2)\, x_2]\; V\, d\theta$$

$$= \int_0^{\theta_2} \left[c_{HS_1} + \frac{\beta_1}{2}\,(D+d) \right] \left[\frac{(d-D)}{\sin(\xi+\theta_1+\theta)} \right]$$

$$[1+(k_1-1)\sin^2(\xi+\theta_1+\theta+\mu)]\; V_0\, e^{(\theta_1+\theta)\tan\varphi}\, d\theta$$

$$+ \int_0^{\theta_2} \left[c_{HS_2}\, x_2 + \frac{\beta_2}{2}\; x_2^2 \sin(\xi+\theta_1+\theta) \right]$$

$$. [1+(k_2-1)\sin^2(\xi+\theta_1+\theta+\mu)]\; V_0\, e^{(\theta_1+\theta)\tan\varphi}\, d\theta \qquad \ldots (8)$$

Rate of energy dissipation along the straight line portion $ef = E_6$

$$E_6 = (\text{average } c_i \text{ along } ef)\,(\text{length } ef)\,(V\cos\varphi)$$

$$= \frac{BV_0}{2\cos\xi}\, e^{(\theta_1+\theta_2)\tan\varphi}\, \frac{2\sin\theta_3}{\cos(\varphi+\theta_3)}\, \cos\varphi \left\{ c_{HS_2} \right.$$

$$\left. + \frac{\beta_2}{2} \left[\frac{B}{2\cos\xi}\, \frac{e^{(\theta_1+\theta_2)\tan\varphi}}{\sin(\xi+\theta_1+\theta_2)} - (d-D) \right] \right\}$$

$$. [1+(k_2-1)\sin^2(\theta_2-Y)] \qquad \ldots (9)$$

Rate of energy dissipation along $fg = E_7$

$$E_7 = (\text{average } c_i \text{ along } fg)\,(\text{length } fg)\,(V\cos\varphi)$$

$$= \frac{BV_0\, e^{2(\theta_1+\theta_2)\tan\varphi} \sin(\eta-\theta_3)\cos^2\varphi}{2\cos\xi\,\cos(\varphi+\theta_3)\,\cos(\varphi+\eta)} \left[c_{HS_1} + \frac{\beta_1\, d}{2} \right]$$

$$. [1+(k_1-1)\sin^2(\theta_2-Y)] \qquad \ldots (10)$$

Half of rate of work done due to weight of soil in triangle $abc = E_8$

$$E_8 = \frac{1}{8} \frac{\gamma_1 B^2 V_0 \sin \xi \cos \varphi}{\cos \xi \cos (\xi - \varphi)} \qquad \dots (11)$$

Rate of work done due to weight of soil in logarithmic spiral $bcd = E_9$

$$E_9 = \frac{\gamma_1 B^2 V_0}{8 \cos^2 (1+9 \tan^2 \varphi)} \{e^{3\theta_1 \tan \varphi} [3 \tan \varphi \cos (\xi - \theta_1)$$
$$+ \sin (\xi + \theta_1)] - 3 \tan \varphi \cos \xi - \sin \xi]\} \qquad \dots (12)$$

Rate of work done due to weight of soil in the logarithmic spiral bde can be considered as the sum of the rates of work done in logarithmic spiral bde with unit weight γ_2 and the difference in the rate of work done in the portion bdf' due to difference in the unit weights. This is obtained as

$$E_{10} = \int_0^{\theta_2} \tfrac{1}{2} \gamma_2 r^2 V \cos (\xi + \theta_1 + \theta)\, d\theta$$
$$+ \int_0^{\theta_2} \tfrac{1}{2} (\gamma_2 - \gamma_1) \left[\frac{d-D}{\sin (\xi + \theta_1 + \theta)}\right]^2 V \cos (\xi + \theta_1 + \theta)\, d\theta \qquad \dots (13)$$

Rate of work done due to weight in portion $befgh$ can be considered as the sum of rates of work done due to weight of soil in portion $befgh$ with unit weight γ_1 and the difference in the rate of work done in portion eff' due to change in unit weight. This is obtained as

$$E_{11} = -\frac{1}{8} \frac{\gamma_1 B^2 V_0}{\cos^2 \xi} \left[\frac{\sin \beta' \cos \beta' \cos^2 \varphi}{\cos^2 (\varphi + \eta)} + \frac{\sin \eta \cos \varphi}{\cos (\varphi + \eta)}\right]$$
$$\cdot [\cos (\eta - \beta')\, e^{3(\theta_1 + \theta_2) \tan \varphi}]$$
$$- \tfrac{1}{2} (\gamma_2 - \gamma_1) \left[\frac{B}{2 \cos \xi} e^{(\theta_1 + \theta_2) \tan \varphi} - \frac{(d-D)}{\sin (\eta - \beta')}\right]^2 \cdot \frac{\cos \varphi}{\cos (\varphi + \eta - \beta')}$$
$$\cdot [\sin (\eta - \beta') V_0\, e^{(\theta_1 + \theta_2) \tan \varphi} \cos (\eta - \beta')] \qquad \dots (14)$$

Rate of work done by the foundation load taking one one half $= E_{12}$

$$E_{12} = q \frac{B}{2} \frac{V_0 \cos \varphi}{\cos (\xi - \varphi)} \qquad \dots (15)$$

Equating the rate of external work done including the rate of work done by the weight of soil (Eqs. 11 to 15), to the rate of energy dissipation (Eqs. 4 to 10), the expression for q can be written as

$$q = (E_1 + E_2 + E_3 + E_4 + E_5 + E_6 + E_7 - E_8 - E_9 - E_{10} - E_{11})$$
$$\cdot \frac{2 \cos (\xi - \varphi)}{B V_0 \cos \varphi} \qquad \dots (16)$$

Referring to Fig. 1, the cohesion at the bottom of top layer is designated as c'_{HS1} and the ratio of (c_{HS2}/c'_{HS1}) as c_R. Introducing the nondimensional variables,

$$\nu_1 = \frac{\beta_1 B}{c_{HS1}},\ \nu_2 = \frac{\beta_2 B}{c_{HS1}},\ G = \frac{\gamma_1 B}{c_{HS1}},\ G_R = \frac{\gamma_2}{\gamma_1},$$

$$d_1 = d/B,\ c_R = c_{HS2}/c'_{HS1}\ ,\ \text{and}\ q' = q/c_{VS},$$

the expression for nondimensional bearing capacity q' can be written as

$$q' = N_c + GN_{\gamma q} \qquad \dots (17)$$

q' is in terms of the above nondimensional parameters. The expressions for N_c and $N_{\gamma q}$ have not been given since they are too lengthy.

For case $1B$ (Fig. $2b$), expressions for E_1, E_2, E_3 are same as for case $1A$. Expressions E_4 and E_5 are to be modified using θ'_2 instead of θ_2. θ'_2 is the angle dbe in Fig. 3, and is arrived at by geometry. Expressions for E_6 and E_7 are also to be modified using θ'_3 and taking appropriate value of average cohesion along radial line. Expressions E_8, E_9 are same as in case $1A$. Expressions E_{10} and and E_{11} are also to be modified. Expression for E_{12} is the same as for case $1A$.

For case $2A$ (Fig. $3a$) Eq. 1 is to be modified, E_2 and E_3 are zero since $\theta_1 = 0$. Expressions for E_4, E_5, E_6, E_7, E_9, E_{10} and E_{11} are same as for case $1A$. Expression E_8 is to be suitably modified since the wedge lies in both layers. Expression for E_{12} is the same as for case $1A$.

For case $2B$, expressions E_1 and E_8 are to be modified as above, and expressions for E_2 to E_7 and E_9 to E_{11} are the same as for case $1B$. Expression for E_{12} is the same as for case $1A$.

Similarly, for case 3 expressions for E_1 to E_{11}, are to be suitably modified taking into account appropriate expressions for cohesions along the failure surface and average cohesion. Details of modifications and expressions for the cases discussed are given elsewhere (Venkatakrishna Rao, 1980).

For obtaining q' minimum, ξ and η which define the failure mechanism should satisfy the conditions

$$\partial q'/\partial \xi = 0 \qquad \dots (18)$$

$$\partial q'/\partial \eta = 0 \qquad \dots (19)$$

Substituting the values of ξ and η which satisfy Eqs. 18 and 19, in the appropriate expression for q', q' minimum is obtained.

Results and Discussions

Numerical values of minimum q' have been obtained for $\varphi = 10$, 30 and 40 degrees, $d' = 0.0$ and 1.0, $d_1 = 0.5$, 1.0 and 1.5, $\nu_1 = 0.0$, 0.8 and 1.20, $k_1 = 0.8$, and 2.0, $c_R = 0.25$, 0.75, 1.0 and 1.5. and $G = 0.0$ and 2.0. Since the parameters involved are many, numerical results are presented for $\nu_2 = \nu_1$, $k_2 = k_1$ and $\gamma_2 = \gamma_1$.

For given parameters, φ, d', d_1, the angles ξ and η define the failure mechanism. The appropriate expressions for q' as discussed earlier are used in obtaining the minimum values. Figures 5 to 10 show the variation of q' with c_R for various other parameters. It can be noted that with the assumption of $\nu_2 = \nu_1$, $k_2 = k_1$, and $\gamma_2 \gamma_1$, $c_R = 1$ corresponds to a single layer.

As could be seen from the figures the variation of q' with c_R is almost linear in most of the cases. These figures also reveal that the trend of variation of q' with change in c_R is also similar to those observed by Button (1953), Reddy and Srinivasan (1967) for clays and that of Purushothamaraj Ramiah and Venkatakrishna Rao (1974) for c-φ soils, i.e. for c_R less than one, the bearing capacity is lower or equal to that of upper layer and for c_R greater than one, the bearing capacity is greater than or equal to that of upper layer. The figures also reveal that for $\nu_1 = 0.0$ and $c_R < 1$, as d_1 increases, the bearing capacity q' increases and approaches the values of upper layer. For $\nu_1 = 0.0$ and $c_R > 1$, as d_1 increases, q' decreases and approaches the values of upper layer. But when $\nu_1 \neq 0.0$ and $c_R < 1$, in some cases as d_1 increases, first there is a decrease in q' and then q' increases and approaches the q' of upper layer. Similarly, when $\nu_1 \neq 0.0$ and $c_R > 1$, in some cases as d_1 increases, first there is an increase in q' and then q' decreases. Such a trend can be explained by the fact that q' depends on variation of cohesion in the upper and lower layers and the corresponding lengths of the failure surface.

In order to compare the influence of soil on the bearing capacity, the values of q' obtained for layered case are compared with those of the upper layer extending to infinite depth (called herein as single layer) and the following variations are observed:

(*i*) The change in the bearing capacity when compared to that of single layer is more for $G = 0.0$ than that for $G = 2.0$. For the range of parameters considered in the analysis, the ratio of q' of layered case to q' of single layer varies from 0.304 to 1.490 for $G = 0.0$, and for $G = 2.0$, the variation ranges from 0.491 to 1.328. This is to be expected since anisotropy and nonhomogeneity in cohesion is to affect more the terms contributing to N_c then $N_{\gamma q}$.

(*ii*) For given set of parameters, as k_1 changes from 0.8 to 2.0, change in the ratio is not very much. For the range of other parameters considered, as k_1 changes from 0.8 to 2.0, the maximum change is of the order of -3.0 to 12.5 per cent with respect to $k_1 = 0.8$ values.

(*iii*) As ν_1 changes from 0 to 1.2, the changes in ratios are more compared to the changes due to k_1. For $\varphi = 10$ degrees, as ν_1 changes from 0 to 1.2, the change in ratios range from 86 to -12 per cent with respect to $\nu_1 = 0.0$ case, and for $\varphi = 40$ degrees the range is 118 to -16 per cent.

(*iv*) For given other parameters, d' has considerable influence on the bearing capacity of layered soil. With increase in d', effect of layers is more pronounced, since increase in d' increases the depth of failure surface.

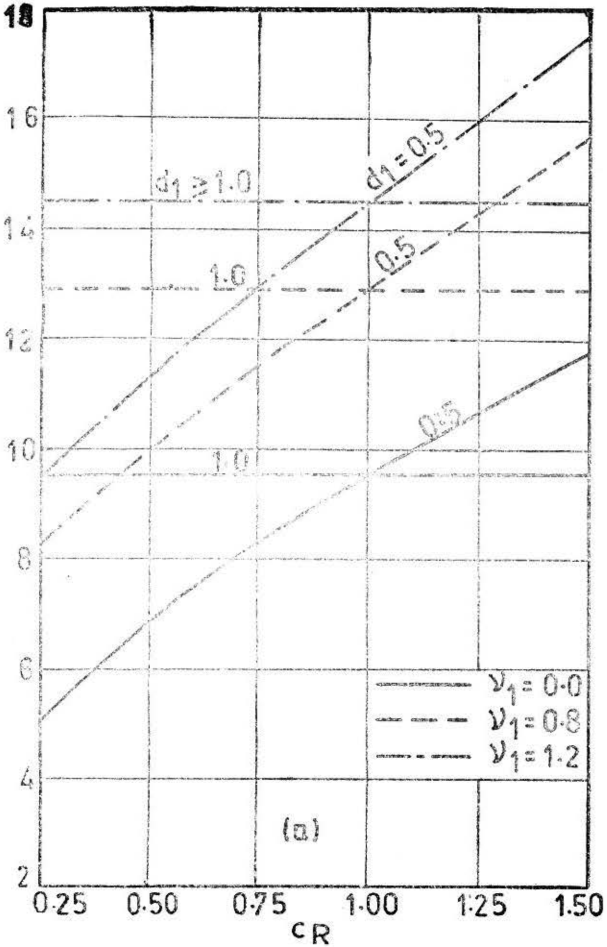

(a) $k_1 = 0.8$, $d' = 0.0$

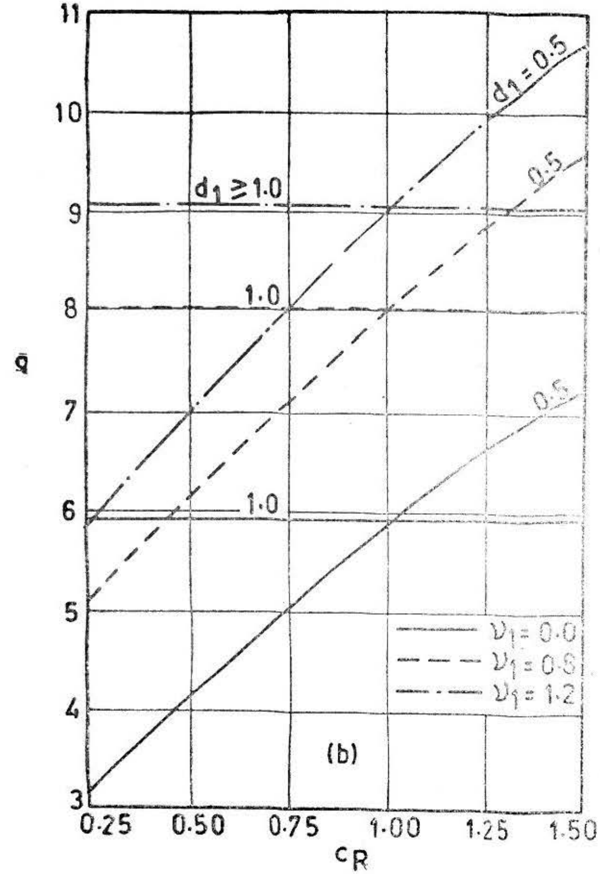

(b) $k_1 = 2.0$, $d' = 0.0$

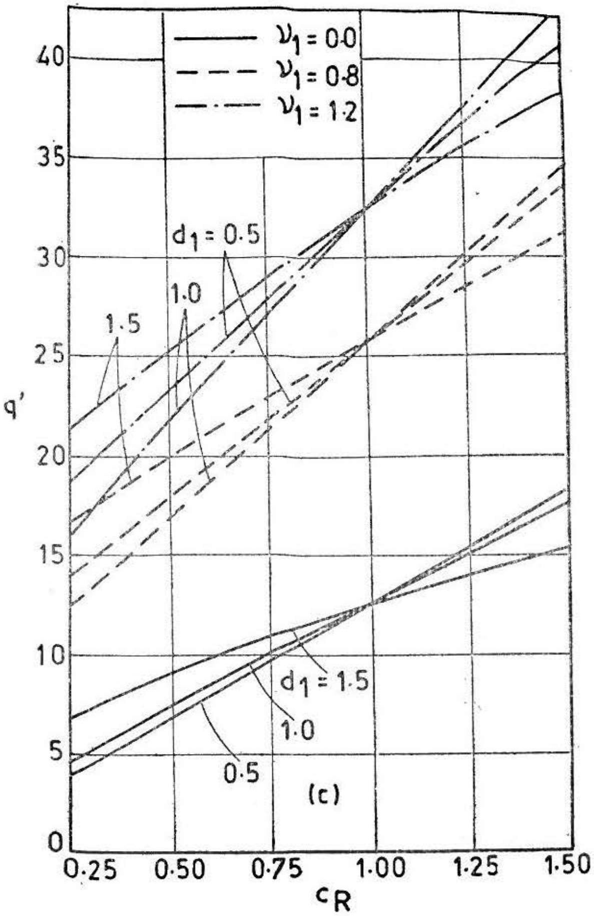

(c) $k_1=0.8$, $d'=1.0$

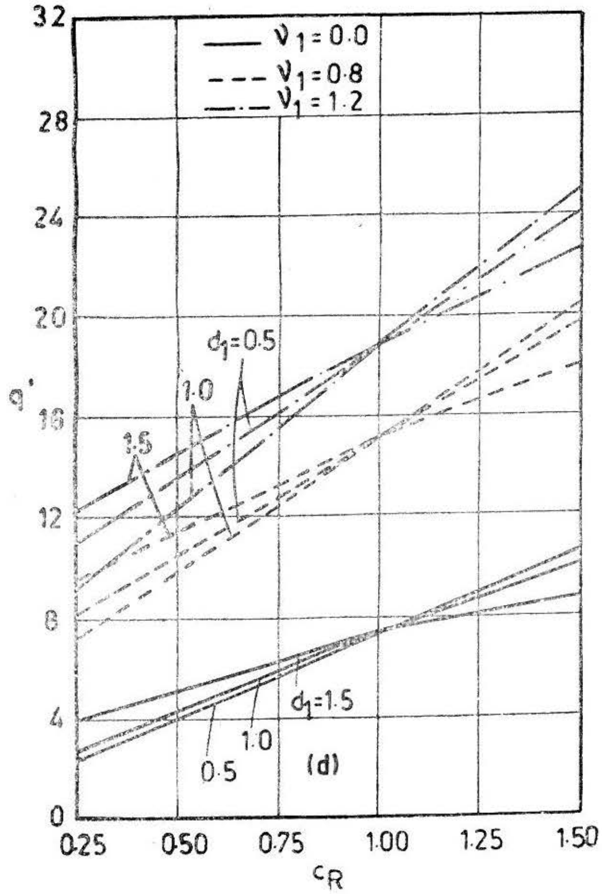

(d) $k_1=2.0$, $d'=1.0$

FIGURE 5. Values of q' for $\phi=10°$, $G=0.0$

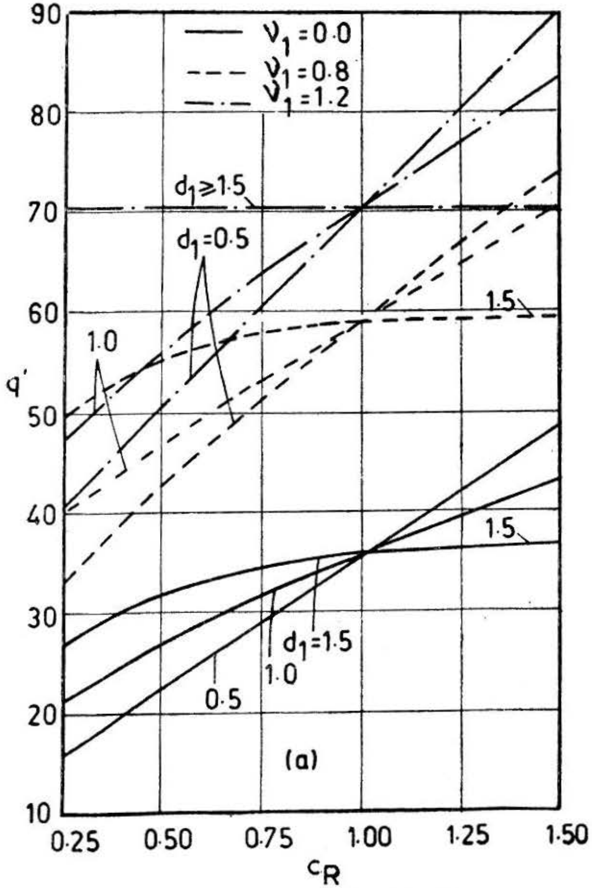

(a) $k_1 = 0.8$, $d' = 0.0$

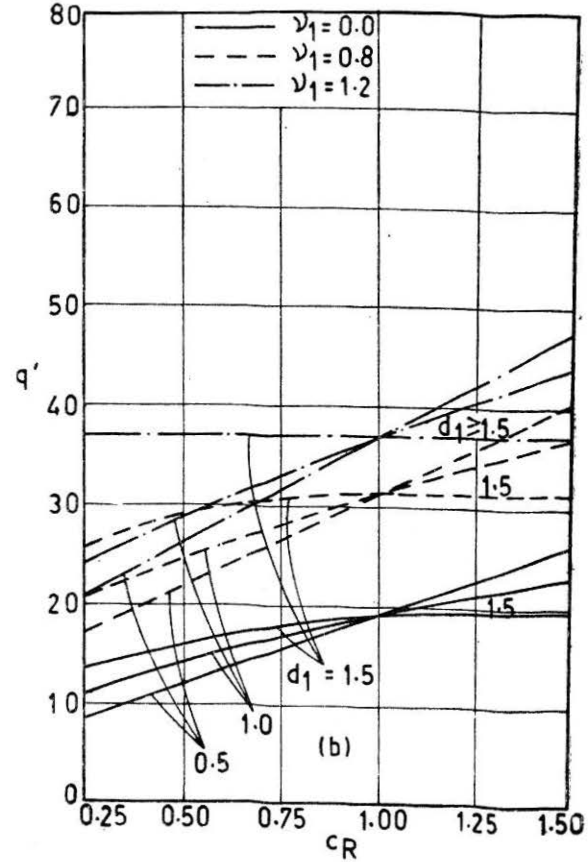

(b) $k_1 = 2.0$, $d' = 0.0$

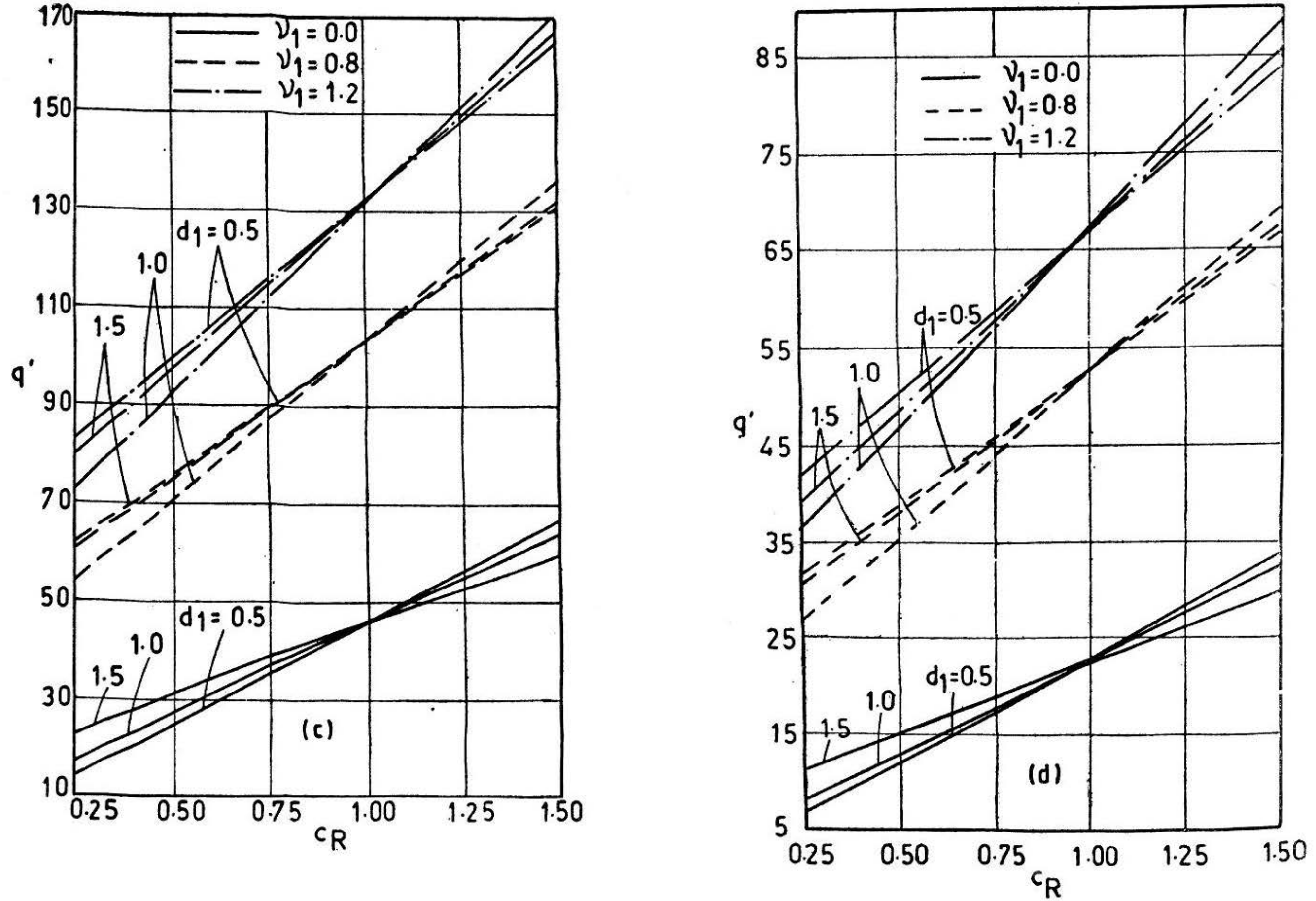

(c) $k_1=0.8$, $d'=1.0$ (d) $k_1=2.0$, $d'=1.0$

FIGURE 6 Values of q' for $\phi=30°$ $G=0.0$

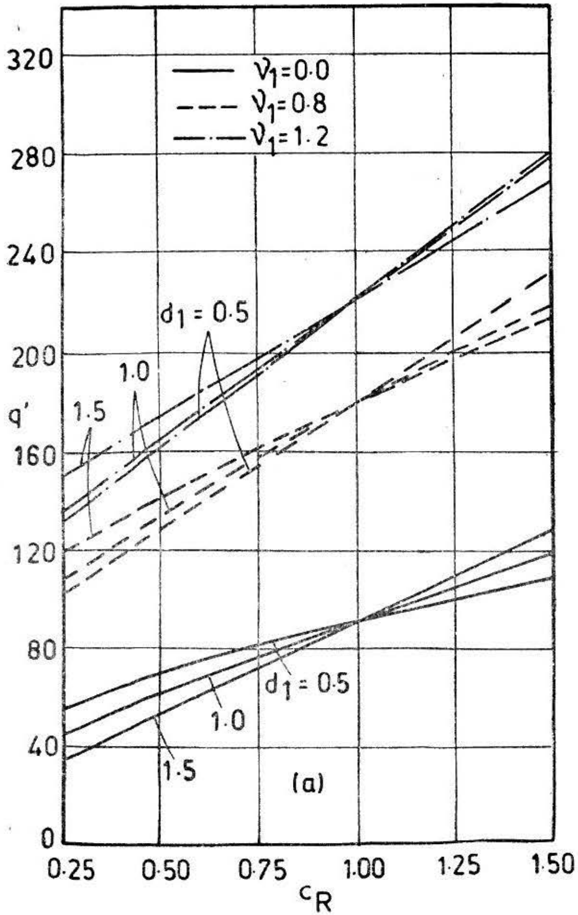

(a) k_1=0.8, d'=0.0

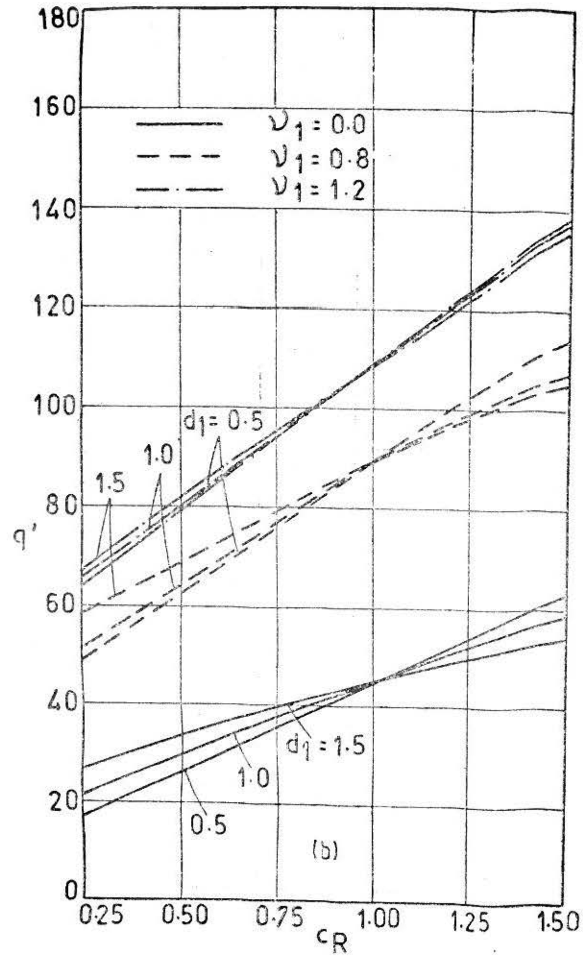

(b) k_1=2.0, d'=0.0

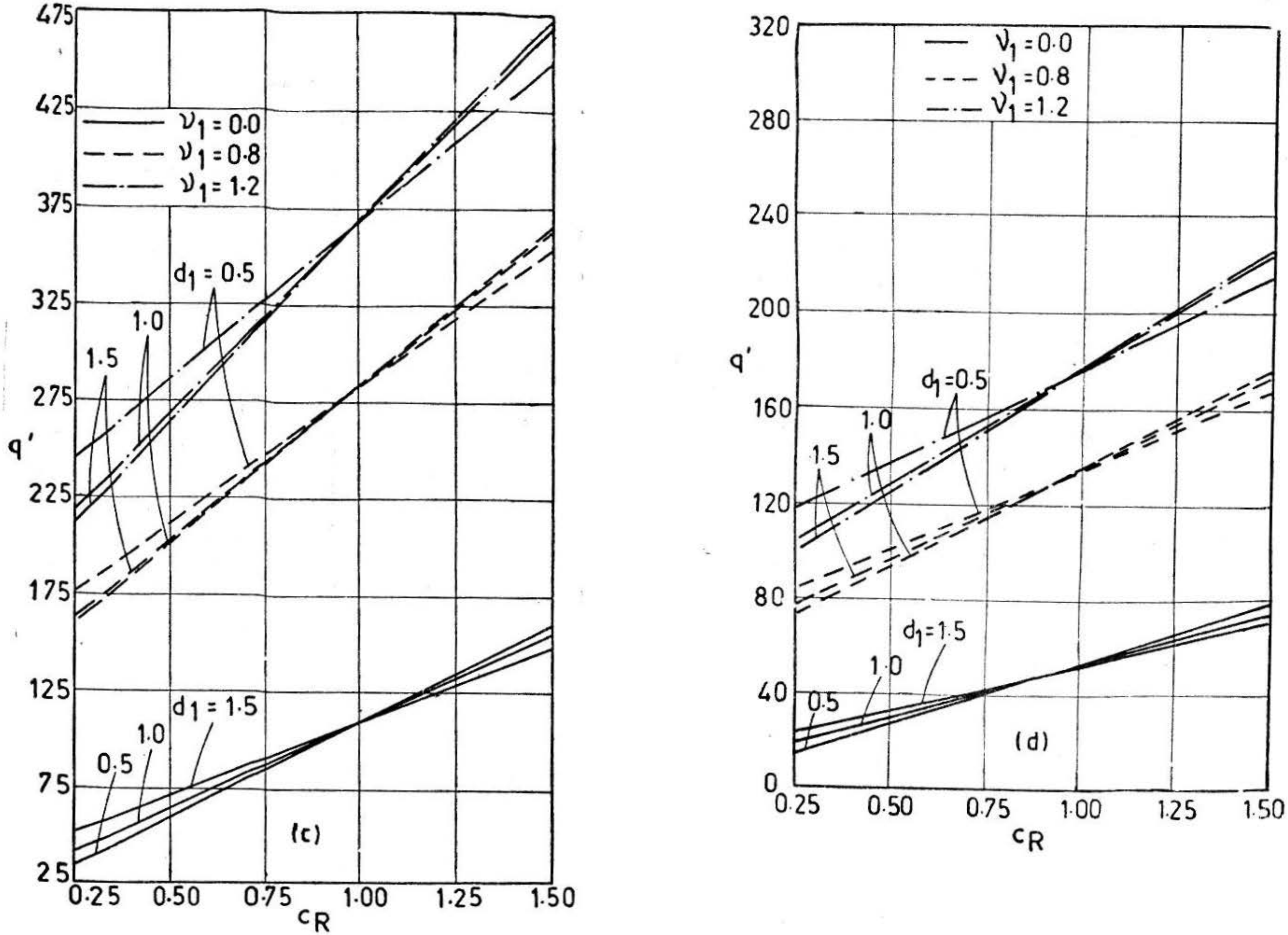

(c) $k_1 = 0.8$, $d' = 1.0$

(d) $k_1 = 2.0$, $d' = 0.0$

FIGURE 7 Values of q' for $\phi = 40°$ $G = 0.0$

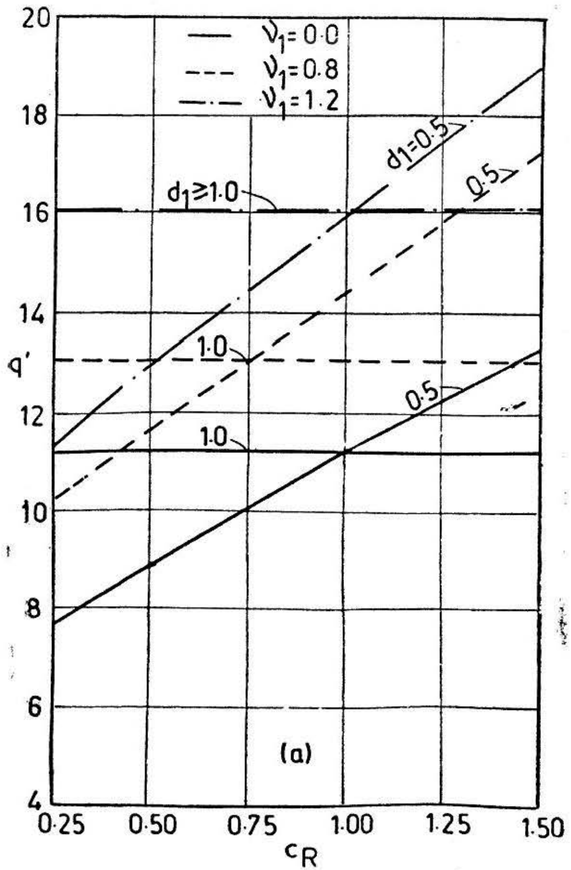

(*a*) $k_1 = 0.8$ $d' = 0.0$

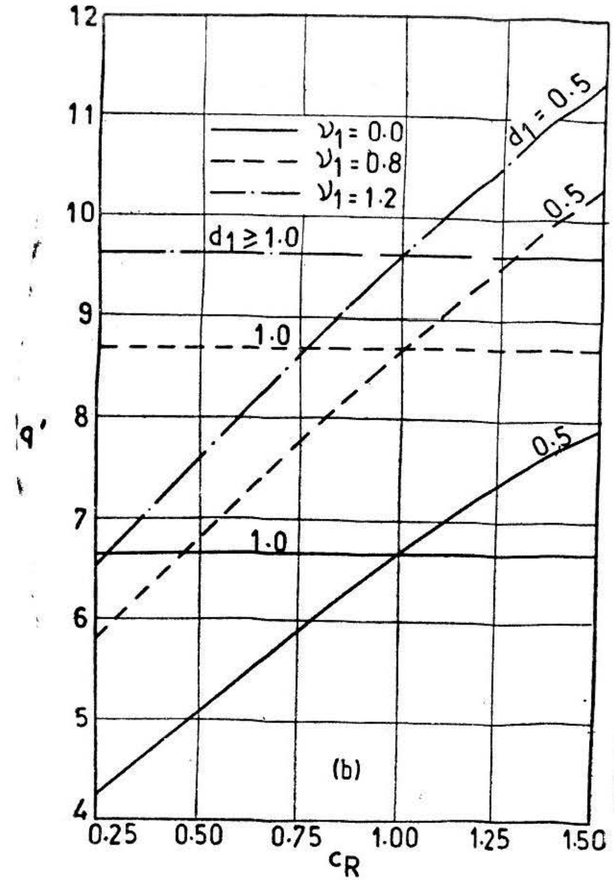

(*b*) $k_1 = 2.0$ $d' = 0.0$

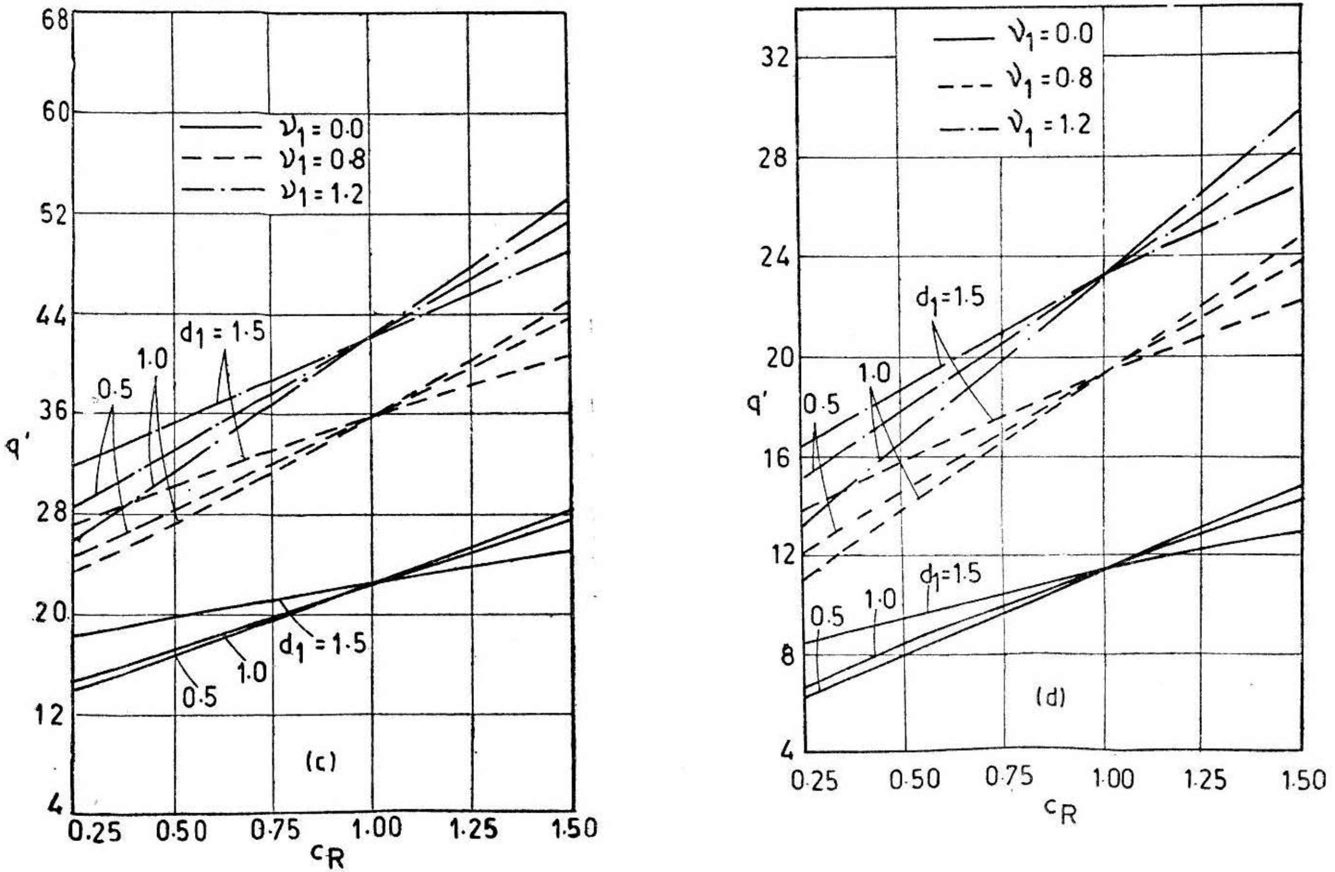

(c) k_1=0.8 d'=1.0 (d) k_1=2.0 d'=1.0

FIGURE 8 Values of q' for $\phi=10°$ $G=2.0$

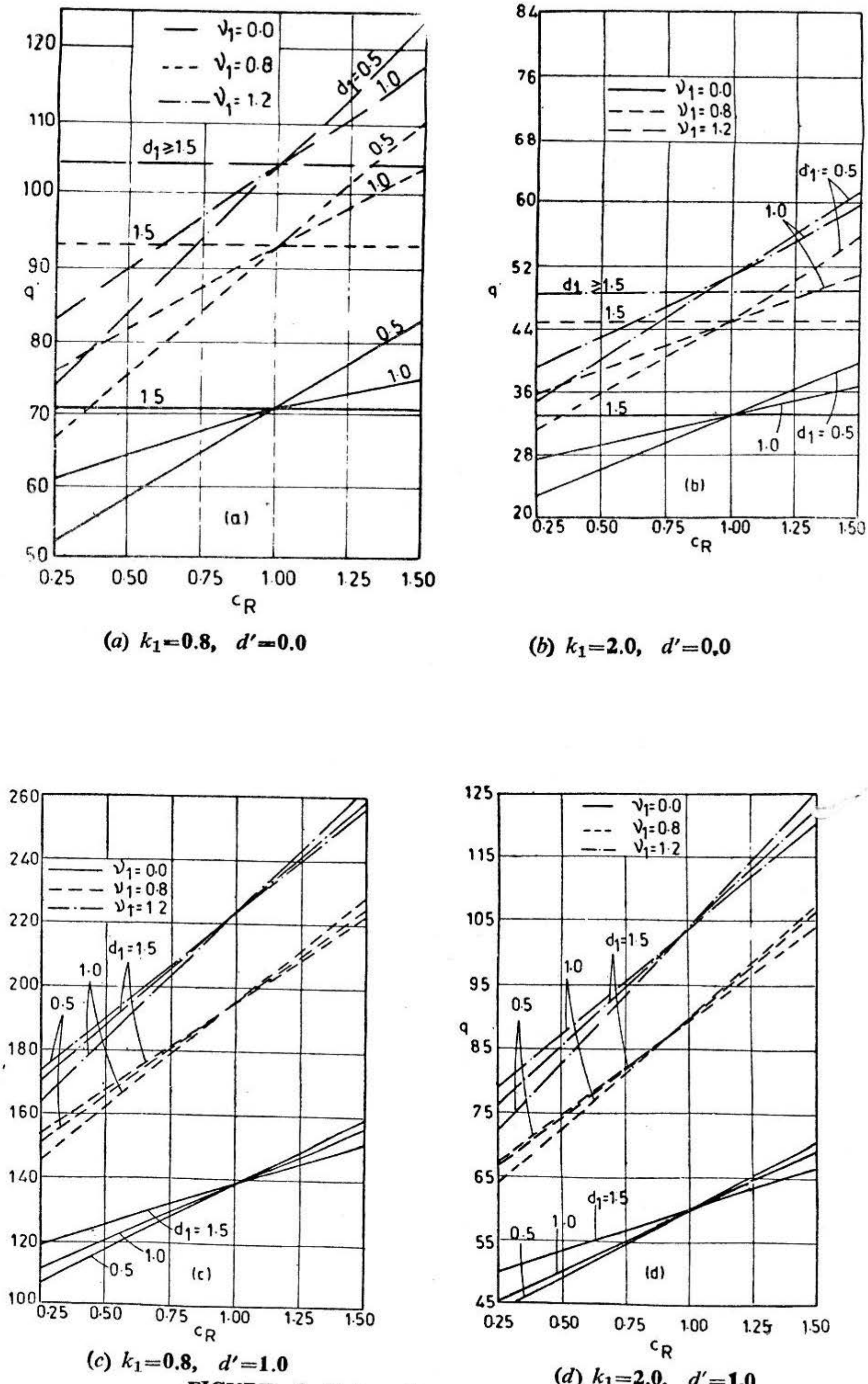

(*a*) $k_1=0.8$, $d'=0.0$

(*b*) $k_1=2.0$, $d'=0.0$

(*c*) $k_1=0.8$, $d'=1.0$

(*d*) $k_1=2.0$, $d'=1.0$

FIGURE 9 Values of q' for $\phi=30°$ $G=2.0$

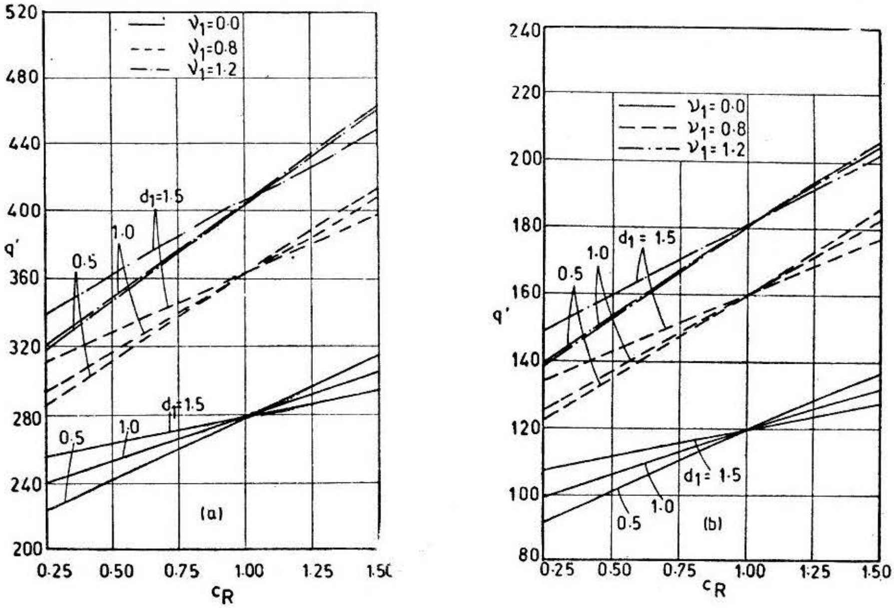

(*a*) k_1=**0.8**, d'=**0.0** (*b*) k_1=**2.0**, d'=**0.0**

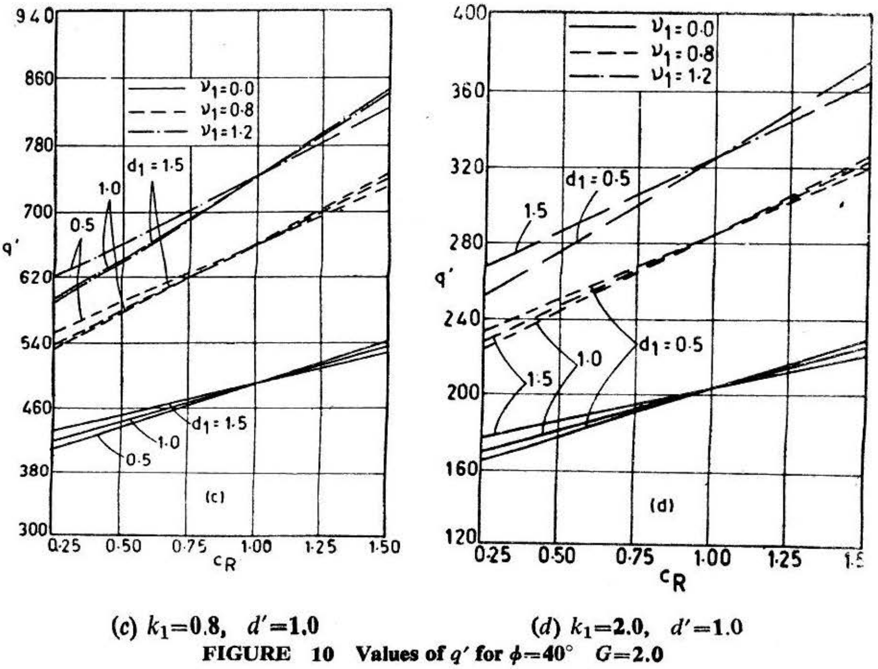

(*c*) k_1=**0.8**, d'=**1.0** (*d*) k_1=**2.0**, d'=**1.0**

FIGURE 10 Values of q' **for** ϕ=**40°** G=**2.0**

(*v*) As φ increases, the maximum depth of failure surface increases and hence values of d_1 that influence the bearing capacity also increase.

(*vi*) When $c_R < 1$, the bearing capacity of layered soil is less than or equal to the bearing capacity of single layer. When $c_R > 1$, the bearing is greater than or equal to the bearing capacity of single layer. Also, it is observed that the effect of c_R is more for $G=0.0$ compared to $G = 2.0$.

(*vii*) The effect of increase in d_1 is to reduce the effect of layers on the bearing capacity. Again, the changes in q' as d_1 increases is more for $G=0.0$ compared to $G = 2.0$.

(*viii*) For the range of parameters considered, the ratio of q' layered to q' single layer varies from 0.30 to 1.490,

In order to study the influence of anisotropy and nonhomogeneity in each layer, the ratios of bearing capacity of the layered system considering anisotropy and nonhomogeneity in each layer and the bearing capacity of layered system treating each layer as homogeneous and isotropic are obtained. The details of these are given elsewhere (Venkatakrishna Rao, 1980). For the range of parameters considered, these ratios vary from 0.505 to 8.85.

The failure surfaces for which q' minimum is obtained, vary with change in parameters such as ν_1, k_1, c_R and other parameters. The typical failure surfaces are shown in Fig. 11. As could be seen from this figure, with increase in ν_1 or k_1, the failure surface becomes shallower and narrower. It can also be seen that as c_R increases, the failure becomes shallower and narrower.

Conclusions

Anisotropy and nonhomogeneity in cohesion in each layer have considerable influence on the ultimate bearing capacity. For the range of parameters considered, the ratio of bearing capacity of layered soil to bearing capacity of top layer extending to infinity varies from 0.30 to 1.490. The ratios of bearing capacity of layered soil treating each layer as anisotropic and nonhomogeneous to that of the same layer treating the soil as homogenous and isotropic vary from 0.50 to 8.85.

References

BISHOP, A.W. (1966), 'The strength of soils as engineering materials', *Geotechnique*, 16:2:89-128.

BROWN, J.D., and MEYERHOF, G.G., (1969), 'Experimental study of bearing capacity of layered, clays', Proc VII ICSMFE 2:45-52.

BUTTON, S.J., (1953), 'The bearing capacity of footings on a two layer cohesive sub-soil', Proc III ICSMFE, Switzerland, : 1: 332-335.

CASAGRANDE, A., AND CARRILO, N., (1944), 'Shear failure of anisotropic materials', *Journal of Boston Society of Civil Engineers*, Reprinted in Contributions to Soil Mechanics, 1941-1953, pp. 127-135.

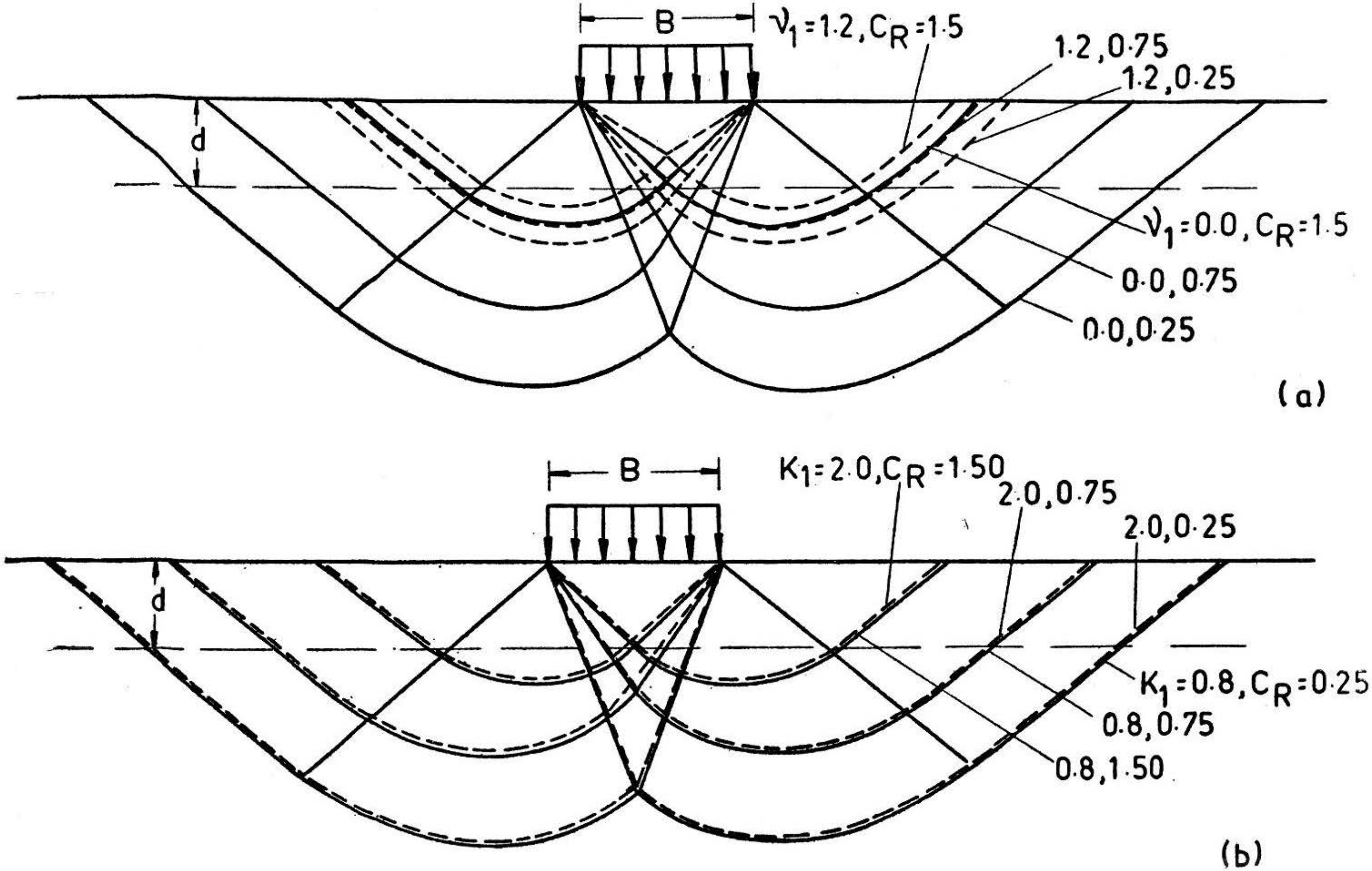

FIGURE 11 (*a*) **Failure Surface for $\phi=10^\circ$, $k_1=0.8$, $d'=0.0$, $d_1=0.5$ and $G=0.0$**
(*b*) **Failure Surfaee for $\phi=10^\circ$, $k_1=0.0$, $d'=0.0$, $d_1=0.5$ and $G=0.0$**

CHEN, W.F., (1975), '*Limit analysis and soil plasticity*', Elsevier Publishing Company, Amsterdam.

HANNA, A.M., and MEYERHOF, G.G., (1979), 'Ultimate bearing capacity of foundations on a three layered sands', *Canadian Geotechnical Journal*,: 16:2: 412-413.

LIVNEH, M., and KOORNIK, A., (1967), 'Anisotropic strength of compacted clays', *Proceedings, Third Asian Regional* Conf SMFE Israel; 1: 298-304.

LO, K.Y., (1965), 'Stability of slopes in anisotropic soils', JSMFED ASCE: 91: SM4: 85-106.

MEYERHOF, G.G. (1974), 'Ultimate bearing capacity of footings on sand layer overlying clay', *Canadian Geotechnical Journal*: 11: 2: 223-229.

MEYERHOF, G.G., and HANNA, A.M., (1978), 'Ultimate bearing capacity of foundations on layered soils under inclined load', *Canadian Geotechnical Journal*: 15: 4: 545-572.

PURUSHOTHAMARAJ, P., RAMIAH, B.K. and VENKATAKRISHNA RAO, K.N., (1974), 'Bearing capacity of strip footing in two layer cohesive friction soils', *Canadian Geotechnical Journal*: 11: 1: 32-45.

REDDY, A.S., and SRINIVASAN, R.J., (1967), 'Bearing capacity of footings on layered clays', JSMFED, ASCE: 93: SM2: 83-99.

STRAGNOV, A.S., (1967), 'Foundaiion stability on unstabilized sub-soil', Proc. III Asian Regional Conf SMFE, Israel, pp. 15-22.

VENKATAKRISHNA RAO, K.N., (1980), 'Ultimate bearing capacity and stability of slopes considering anisotropy and nonhomogeneity in cohesion and other related stability problems', Ph. D. Thesis submitted to the Indian Institute of Science, Bangalore, India.

VESIC, A.S., (1975), 'Bearing capacity of shallow foundations,' Foundation Engineering Hand Book, Ed. Wintercorn and Fang, *von Nostrand Reinhold Company*, New York, U.S.A., pp. 121-147.

YAMAGUCHI, H., (1963), 'Practical formulae for bearing capacity of two layered ground', Proc II Asian Regional Conf, SMFE : 1: 176-178.

Notation

B	=	width of foundation;
c	=	cohesion of soil;
c_H	=	cohesion in the horizontal direction;
c_{HS1}	=	cohesion at surface in the horizontal direction of top layer;
c_{HS2}	=	cohesion at the top of lower layer in the horizontal direction;
c'_{HS1}	=	cohesion at the bottom of top layer;
c_{VS}	=	cohesion at surface in the vertical direction;
c_R	=	c_{HS2} / c'_{HS1};
c_V	=	cohesion in the vertical direction;

c_i	=	cohesion corresponding to an inclination i of the major principal stress with horizontal;
D	=	depth of foundation;
d	=	thickness of top layer;
d_1	=	d/B;
d'	=	D/B;
E_1 to E_{12}	=	expressions for rates of energy dissipation and external work done for different portions;
G	=	$\gamma_1 B/c_{HSL}$;
G_R	=	γ_2/γ_1;
i	=	inclinations of direction of major principal stress with horizontal;
k_1, k_2	=	coefficients of anisotropy in the top and lower layers, respectively $= c_V/c_H$;
$N_C, N_{\gamma q}$	=	nondimensional bearing capacity factors;
q	=	ultimate bearing capacity;
q'	=	nondimensional bearing capacity $= q/c_{VS}$;
r	=	radius of the logarithmic spiral;
V_1	=	vertical velocity (Fig, 2a);
V_O, V_r	=	relative velocities (Fig. 2a);
x_1, x_2	=	portions of length of radial line in the top and lower layers, respectively;
β_1	=	variation of cohesion with depth in top layer;
β_2	=	variation of cohesion with depth on the lower layer;
β'	=	angle as shown in Figs. 2 to 5;
γ_1, γ_2	=	unit weights of soil in the top and lower layers, respectively;
η	=	boundary wedge angles, shown in Figs. 2 to 5;
θ	=	angle made by radial line with vertical;
θ_1	=	angle bed in Figs. 2(a) and 3(a);
θ_2	=	angle as shown in Figs. 2 (a), 3(a) and 4;
θ_3	=	angle shown in Figs. 2(a) and 3(b) and 4;

θ'_2, θ'_3 = angles as shown in Fig. 2(*b*) and 3(*b*);

μ = $45° - \phi/2$;

ν_1 = $\beta_1 B/c_{HS1}$;

ν_2 = $\beta_2 B/c_{HS1}$;

ξ = angle made by the triangular wedge at the base of foundation (see Figs 2 to 4)

φ = angle of internal friction of soil.